Article

Optical Floating Zone Crystal Growth of Rare-Earth Disilicates, R₂Si₂O₇ (R = Er, Ho, and Tm)

Monica Ciomaga Hatnean,* Oleg A. Petrenko, Martin R. Lees, Tom E. Orton, and Geetha Balakrishnan

Read Online

ACCESS | Metrics & More | Article Recommendations

ABSTRACT: The wealth of structural phases seen in the rare-earth disilicate compounds promises an equally rich range of interesting magnetic properties. We report on the crystal growth by the optical floating zone method of members of the rare-earth disilicate family, $R_2Si_2O_7$ (with R = Er, Ho, and Tm). Through a systematic study, we have optimized the growth conditions for $Er_2Si_2O_7$. We have grown, for the first time using the floating zone method, crystal boules of $Ho_2Si_2O_7$ and $Tm_2Si_2O_7$ compounds. We show that the difficulties encountered in the synthesis of polycrystalline and single crystal samples are due to the similar thermal stability ranges of different rare-earth silicate compounds in the temperature−composition phase diagrams of the R-Si-O systems. The addition of a small amount of SiO_2 excess allowed the amount of impurity phases present in the powder samples to be minimized. The phase composition analysis of the powder X-ray diffraction data collected on the as-grown boules revealed that they were of single phase, except in the case of thulium disilicate, which was comprised of two phases. All growths resulted in multigrain boules, from which sizable single crystals could be isolated. The optimum conditions used for the synthesis and crystal growth of polycrystalline and single crystal $R_2Si_2O_7$ materials are reported. Specific heat measurements of erbium and thulium disilicate compounds confirm an antiferromagnetic phase transition below $T_N = 1.8$ K for D-type $Er_2Si_2O_7$ and a Schottky anomaly centered around 3.5 K in C-type $Tm_2Si_2O_7$, with an upturn in $C(T)/T$ below 1 K suggesting the onset of short-range magnetic correlations. Magnetic susceptibility data of E-type $Ho_2Si_2O_7$ reveals an antiferromagnetic ordering of the Ho spins below $T_N = 2.3$ K.
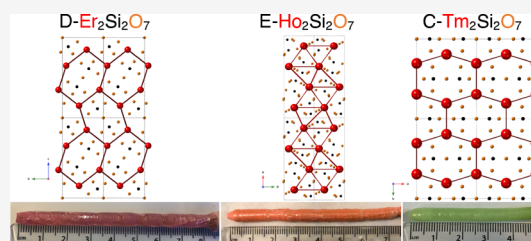
INTRODUCTION

Rare-earth disilicates, $R_2Si_2O_7$, where R is a rare-earth element, were studied in the past due to the polymorphism exhibited by these compounds and their physical properties. At ambient pressure, $R_2Si_2O_7$ compounds can crystallize in seven different structural types.[1−3] The seven polymorphs, conventionally referred to as A, B (or α), C (or β), D (or γ), E (or δ), F, and G, have, respectively, tetragonal ($P4_1$), triclinic ($P\bar{1}$), monoclinic ($C2/m$), monoclinic ($P2_1/a$), orthorhombic ($Pnam$ or $Pna2_1$), triclinic ($P\bar{1}$), and monoclinic ($P2_1/c$) crystal structure.[2] At room temperature and ambient pressure, $R_2Si_2O_7$ compounds can be stabilized in one of three of these structures, depending on the ionic radius of the rare-earth element, R. Rare-earth disilicate compounds containing large rare-earth elements (with R = La → Sm) crystallize in the tetragonal A-type structure. Compounds $R_2Si_2O_7$ that incorporate smaller rare-earth ions (where R = Eu → Tm) adopt a triclinic B-type structure. The smallest rare-earth elements, Lu and Yb, form disilicate compounds crystallizing in the monoclinic C-type structure. At high temperature (950 ≲ T ≤ 1500 °C), rare-earth disilicate compounds $R_2Si_2O_7$ (where R = La → Tm) undergo one or more structural phase transitions. The number of phase transitions they undergo and their transition temperatures depend on the nature of the rare-earth ion.[2] A detailed diagram describing the thermal area of

stability of the polymorphs, as well as the characteristics of each crystallographic structure, for each rare-earth disilicate compound, can be found in the early work of Felsche.[2] Two new polymorphs, K and L, with monoclinic ($P2_1/n$) and triclinic ($P\bar{1}$) crystal symmetries, were later synthesized under pressure.[4]

$R_2Si_2O_7$ compounds are widely investigated for their luminescent and optical properties, with potential applications as crystal scintillators and in the detection of γ- and X-rays.[5−9] Recently, rare-earth disilicates were identified as promising candidates for thermal barrier coating/environmental barrier coating systems, due to their low thermal conductivities.[10−15]

Other properties, such as the magnetic behavior of $R_2Si_2O_7$ compounds, have not been investigated in great detail, partly due to the complexity of the structural phase diagram. The successful growth of ytterbium and erbium disilicate crystals using the optical floating zone (FZ) method[16] has resulted in a

resurgence of interest in the magnetic ground states of these compounds.[17,18] $Yb_2Si_2O_7$ is the first Yb^{3+} based material that exhibits a quantum dimer magnet state, consisting of nearest neighbor spin dimers, with magnetic field-induced order reminiscent of a Bose–Einstein condensate phase. Ytterbium disilicate is one of the very few $R_2Si_2O_7$ compounds that crystallizes in only one structural type,[2] whereas for the other members of the rare-earth disilicate compounds stabilizing in two or more crystallographic structures, extensive studies of the magnetic properties are scarce in the literature.

The growth of $R_2Si_2O_7$ crystals opens up a route to further investigation of these materials, with the potential to unearth some very interesting magnetic properties, similar to what has been observed in $Yb_2Si_2O_7$. There have been many attempts to grow crystals of the rare-earth disilicate compounds. Typical routes used to prepare $R_2Si_2O_7$ crystals include the Verneuil,[19] flux,[20−25] Czochralski,[8] chemical vapor transport,[26] floating zone,[6,16] and micropulling-down[27] techniques. The FZ method of crystal growth has been widely employed in the past for the growth of oxides, and not only is it an ideal technique to produce large, high-quality single crystals, but it is also one of the most appropriate methods due to its advantages compared to the conventional techniques of crystal growth.[28−30] The main benefits of employing the standard FZ technique for the growth of crystals are (a) the high purity of the crystals grown thanks to the absence of a container (crucible) and solvent (flux), (b) the relatively large size of the crystal boules obtained compared with other techniques, (c) the good crystalline quality and uniformity of the physical properties throughout the crystals, (d) the fact that this method can be used for growing refractory materials.

This has motivated us to embark upon the study of the highly polymorphic rare-earth disilicate compounds. In the present work, we investigate three rare-earth disilicate compounds, $R_2Si_2O_7$, where R = Er, Ho, and Tm, with a focus on the crystal growth of these materials using the optical FZ method. $Tm_2Si_2O_7$ is dimorphic with temperature, whereas $Er_2Si_2O_7$ and $Ho_2Si_2O_7$ display a high degree of polymorphism.[2,9,24,25,31−33] A list of the various polymorphs of the disilicate compounds under investigation in this study along with the temperature ranges of their formation/stability, and their respective crystal structures and melting points is given in Table 1.

Rare-earth disilicate compounds have previously been grown in crystal form using the flux method;[20−25] however, the temperature regions where only one crystallographic phase form is narrow and small differences (of 50−100 °C) in the

soak temperature could result in a yield of crystals of two different polymorphs or in a different structural phase to the one desired.[31,33] Previous studies[34,35] of other materials that undergo thermally induced structural phase transitions have proven that the stabilization of a specific structural type is feasible in FZ grown crystals. The crystal growth of the polymorphs of the rare-earth disilicate compounds that are stable at high temperature is therefore made possible by the FZ method, especially for those structural types where the melting points ($1700 \leq T_m \leq 1800$ °C) are higher than the temperatures of the structural phase transitions ($950 \lesssim T \leq 1500$ °C).[2]

Erbium disilicate exists in three polymorphs (see Table 1), a triclinic ($P\bar{1}$) low temperature phase (referred to as B-type), a monoclinic ($C2/m$) structure (C-type), and a high temperature monoclinic ($P2_1/b$) arrangement (D-type).[2,31,32] C-type $Er_2Si_2O_7$ is reported to order antiferromagnetically below $T_N = 2.50(5)$ K.[22,24] The structural modification stable at high temperature, D-type, is one of the most studied polymorphs of $Er_2Si_2O_7$, from a magnetic point of view.[36,37] Furthermore, the C → D-type structural phase transition occurs at a lower temperature ($T_{C \to D} \approx 1425$ °C) than the melting point ($T_m \approx 1750$ °C) (as shown by Felsche,[2] all $R_2Si_2O_7$ compounds do not melt below 1700 °C). A crystal of $Er_2Si_2O_7$ grown from the melt, by the FZ method will therefore belong to the structural type D.[16] Because of the arrangement of the magnetic ions in the crystallographic structure, forming a distorted honeycomb-like lattice (see Figure 1c), one expects to observe interesting magnetic behavior in D-type $Er_2Si_2O_7$, similar to the case of C-type $Yb_2Si_2O_7$.[16−18] Previous reports have shown that D-type $Er_2Si_2O_7$ orders antiferromagnetically below $T_N = 1.9(1)$ K, as well as exhibiting a highly anisotropic magnetic behavior.[36,37] In addition, these first measurements of the magnetic properties suggest that the application of a strong magnetic field induces a "spin flip"; one or two "flips" are observed depending upon the direction of the applied magnetic field. Detailed investigations are required to determine the magnetic ground state of D-type $Er_2Si_2O_7$ and to confirm the four-sublattice antiferromagnetic spin model used for calculating the exchange interaction constants in the initial studies.

Holmium disilicate exists in four polymorphs (see Table 1), two low temperature phases (triclinic B-type arrangement, and monoclinic C-type structure), and two high temperature arrangements (monoclinic D-type phase, and an orthorhombic ($Pna2_1$) E-type structure).[2,33] The temperatures of the structural phase transitions are close to one another in the low temperature region ($T_{B \to C} \approx 1200$ °C, and $T_{C \to D} \approx 1275$ °C),[2] and one can thus expect the synthesis of the low temperature structural types of $Ho_2Si_2O_7$ to be challenging. A study by Maqsood[33] showed that the synthesis attempts carried out in the intermediate temperature region ($1350 \leq T \leq 1400$ °C) can yield more than one crystallographic type of $Ho_2Si_2O_7$ (coexistence of B-type and C-type structures in the materials synthesized). Since holmium disilicate does not melt below 1750 °C,[2] it is expected that a crystal of $Ho_2Si_2O_7$ grown using the FZ method should crystallize in the structural type stable at the highest temperature, i.e., E-type. To date, the magnetic properties of the various polymorphs of holmium disilicate have not been reported.

Thulium disilicate is dimorphic with temperature (see Table 1), the structure stable at low temperature belongs to the B-type, whereas the high temperature polymorph is C-type.[2] Analogous to $Er_2Si_2O_7$ and $Ho_2Si_2O_7$, the melting point ($T_m \approx$

Table 1. Melting Points and Regions of Thermal Stability[2] of Each Polymorph of the $R_2Si_2O_7$ (with R = Er, Ho, and Tm) Compounds

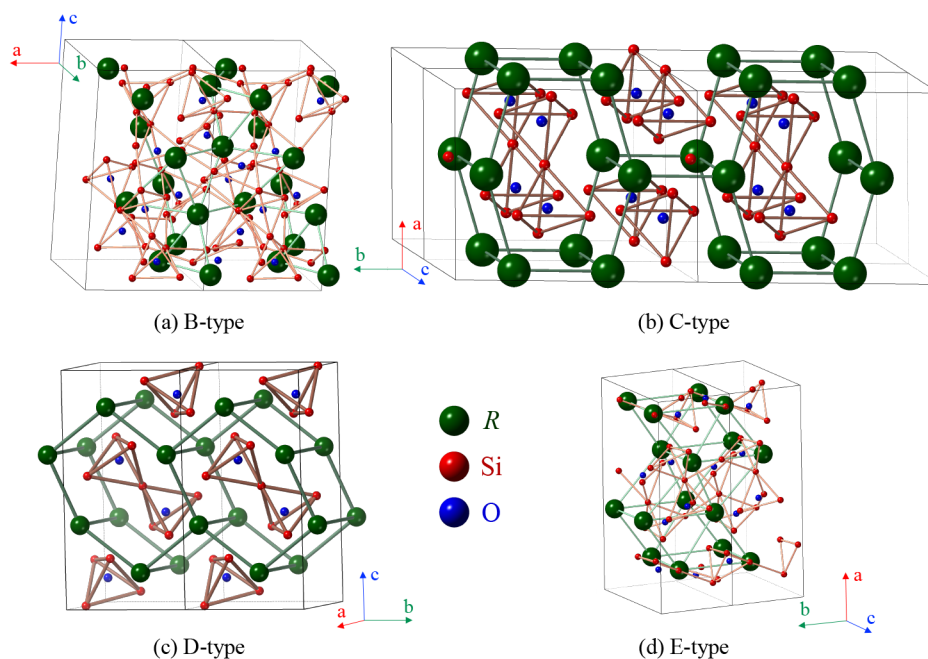| $R_2Si_2O_7$	polymorph	space group	thermal stability range	melting point (T_m)
$Er_2Si_2O_7$	B-type	$P\bar{1}$	$T \lesssim 1025$ °C	~1750 °C
	C-type	$C2/m$	$1025 \lesssim T \lesssim 1425$ °C	
	D-type	$P2_1/b$	$T \geq 1350$ °C	
$Ho_2Si_2O_7$	B-type	$P\bar{1}$	$T \lesssim 1200$ °C	~1750 °C
	C-type	$C2/m$	$1200 \leq T \lesssim 1275$ °C	
	D-type	$P2_1/b$	$1275 \lesssim T \leq 1500$ °C	
	E-type	$Pna2_1$	$T \geq 1500$ °C	
$Tm_2Si_2O_7$	B-type	$P\bar{1}$	$T \lesssim 950$ °C	~1700 °C
	C-type	$C2/m$	$T \gtrsim 950$ °C	

Figure 1. Possible crystallographic structures of the $R_2Si_2O_7$ polymorphs for R = Er, Ho, and Tm: (a) triclinic ($P\bar{1}$) B-type, (b) monoclinic ($C2/m$) C-type, (c) monoclinic ($P2_1/b$) D-type, (d) orthorhombic ($Pna2_1$) E-type. The unit cells are shown in black. The bonds between the magnetic R^{3+} ions emphasize the formation of the distorted honeycomb layers in the C-type and D-type $R_2Si_2O_7$ structures, stacked along the c axis and a axis, respectively. In the E-type structure, the R^{3+} ions form a distorted triangular network.

1700 °C) of the thulium disilicate is higher than the B → C-type structural phase transition temperature ($T_{B\rightarrow C} \approx 950$ °C), one can presume that the crystallographic structure of a crystal of $Tm_2Si_2O_7$ grown using the FZ method will belong to the C-type polymorph. The magnetic properties of the high temperature C-type thulium disilicate have not yet been studied; nevertheless, due to the similarities between the arrangement of the Tm^{3+} and Yb^{3+} ions in the lattice, it is likely that $Tm_2Si_2O_7$ is likely to exhibit as interesting a magnetic behavior as that observed previously in C-type $Yb_2Si_2O_7$.[16−18]

Crystals of the erbium disilicate have been grown previously using the FZ technique;[16] however, in this study, the results of just one growth, under certain conditions, are presented. The holmium and thulium compounds have only been grown in crystal form using the flux method.[2,20,24,25,32,33] First, we have optimized the crystal growth conditions for $Er_2Si_2O_7$, by performing a number of experiments and varying the growth parameters. We have also extended our study to the crystal growth of $R_2Si_2O_7$ (with R = Ho, and Tm) and have successfully prepared, for the first time, using the optical FZ method, crystals of these rare-earth silicates. The crystals obtained are especially suitable for the investigation of the structural properties and magnetic behavior of these materials. Our study shows that there is a direct correlation between the structural features and the magnetism exhibited.

■ EXPERIMENTAL DETAILS

The starting materials used for the synthesis of $R_2Si_2O_7$ (with R = Er, Ho, and Tm) polycrystalline materials were rare-earth oxides, Er_2O_3, Ho_2O_3 and Tm_2O_3 (all of 99.9% purity), and silica, SiO_2 (99.6%). Crystals of rare-earth silicate compounds were then grown using a double ellipsoidal optical image furnace (NEC SC1MDH-11020, Canon Machinery Incorporated), equipped with two 1.5 kW halogen lamps.

The quality of the crystal boules was investigated using a Laue X-ray imaging system with a Photonic-Science Laue camera. Small quantities of each crystal were then ground, and powder X-ray diffraction measurements were performed to determine the phase purity and to establish the crystallographic structure of the $R_2Si_2O_7$ crystals. It is essential to determine the structural type of each crystal. Room temperature diffractograms were collected on X-ray diffractometers (Panalytical and Bruker) using CuKα_1 and CuKα_2 radiation ($\lambda_{K\alpha1}$ = 1.5406 Å and $\lambda_{K\alpha2}$ = 1.5444 Å), over an angular range 10−70° or 10−90° in 2θ, with a step size in the scattering angle 2θ of 0.013° (Panalytical) and 0.016° (Bruker). The analysis of the X-ray patterns was performed using the Fullprof software suite.[38]

Chemical composition analysis was carried out by energy dispersive X-ray spectroscopy (EDAX) using a scanning electron microscope on pieces cleaved from the $R_2Si_2O_7$ crystal boules.

Magnetic susceptibility measurements as a function of temperature were carried out on a ground piece of the $Ho_2Si_2O_7$ crystal down to 1.8 K in applied magnetic fields of 100 and 1000 Oe using a Quantum Design Magnetic Property Measurement System MPMS-5S superconducting quantum interference device (SQUID) magnetometer.

Heat capacity measurements in zero applied magnetic field at temperatures from 0.5 to 300 K were carried out on $Er_2Si_2O_7$ and $Tm_2Si_2O_7$ crystals in a Quantum Design Physical Property Measurement System (PPMS) with a heat capacity option using a two-tau relaxation method.

■ RESULTS AND DISCUSSION

$Er_2Si_2O_7$. *Polycrystalline Synthesis.* D-type $Er_2Si_2O_7$ was first prepared in polycrystalline form by the conventional solid state synthesis method. Powders of Er_2O_3 and SiO_2 were weighed in stoichiometric amounts, mixed together, and heat treated in air for several days (in three or four steps) at temperatures in the range 1400−1500 °C. The annealed mixture (sample labeled ESO) was reground between each step of the synthesis to ensure good homogeneity and to facilitate the reaction of the starting materials. Nevertheless, even after four steps, each of long duration, a phase composition analysis by powder X-ray diffraction (goodness of fit (GOF) = 1.68) reveals the presence of a small quantity of

a SiO_2 deficient erbium monosilicate impurity phase (see Figure 2). This impurity, B-type Er_2SiO_5 (monoclinic
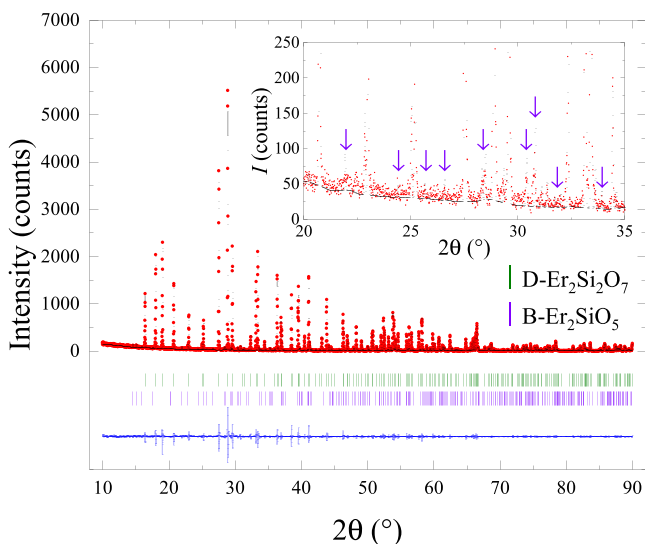

Figure 2. Room temperature powder X-ray diffraction pattern of a $Er_2Si_2O_7$ polycrystalline sample (ESO). The experimental profile (red closed circles) and a full profile matching refinement (black solid line) made using the monoclinic ($P2_1/b$) D-type structure are shown, with the difference given by the blue solid line. The reflections of the D-type $Er_2Si_2O_7$ structure are indicated by green "|", whereas the purple "|" show the reflections belonging to a B-type Er_2SiO_5 (monoclinic $C2/c$ structure) impurity. The inset shows the X-ray pattern in the range 20−35° scattering angle 2θ, with the impurity reflections marked by purple arrows.

structure, $C2/c$),[39] persists even after the powder mixture is annealed at a higher temperature (1550−1600 °C) and/or for extended periods of time (several days). The sintered material was isostatically pressed into rods (typically 6−8 mm diameter and 70−80 mm long) and sintered at 1500−1550 °C in air for several days. The annealed rods were then used for the crystal growth.

Crystal Growth. Crystals of erbium disilicate were grown using the FZ method, in a static air atmosphere, at ambient pressure. In order to optimize the growth conditions, we have carried out a systematic study, by varying the growth speeds and the rotation rates of the two rods (feed and seed). The crystal growths were carried out at growth rates in the range 5−12 mm/h, and the feed and seed rods were counter-rotated, each at a rate of 10−25 rpm. Initially, a polycrystalline rod was used as a seed, and once a good quality crystal boule was obtained, a crystal seed was used for subsequent growths. $Er_2Si_2O_7$ appears to melt congruently, and no deposition was observed on the quartz tube surrounding the feed and seed rods. The best quality crystals (assessment based on the analysis of the X-ray Laue diffraction) were obtained when growth rates of ~10−12 mm/h were employed. The crystal quality appears to be independent of the rotation rate used for the seed rod.

$Er_2Si_2O_7$ crystal boules prepared were typically 4−6 mm in diameter and 70−85 mm long. The boules tended to have thermally generated cracks in most cases, regardless of the growth rate employed. The crystals developed facets as they grew, and two very strong facets were present on more than half the length of the grown crystals. All the erbium disilicate boules were a cloudy pink color. The crystal boules of erbium

disilicate are very fragile, and all the crystals broke along the crystal growth axis into two long halves. Moreover, these two pieces cleaved a second time, perpendicular to the growth axis, thus forming crystal fragments of ~5 × 5 × 3 mm³. Figure 3 shows a photograph of a crystal of $Er_2Si_2O_7$, which was grown using the optimal growth conditions, in air atmosphere, and at a growth speed of 12 mm/h.
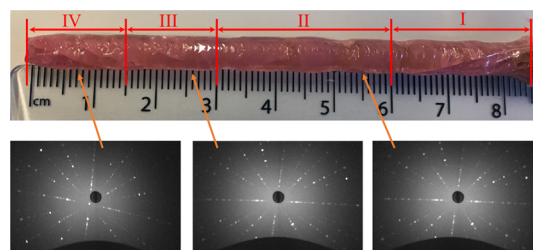

Figure 3. Boule of $Er_2Si_2O_7$ prepared by the floating zone method in an air atmosphere at a growth rate of 12 mm/h. Also shown are the X-ray Laue patterns, taken on one side of the boule at three points along its length. The crystal quality of each of the regions I−IV is discussed in the text.

X-ray Laue photographs taken of boules of $Er_2Si_2O_7$ confirm the good quality of the crystals. Typically, 2−3 grains are present, and they extend along the length of each of the boules. A selection of Laue photographs taken along the length of an $Er_2Si_2O_7$ crystal boule is shown in Figure 3. When a polycrystalline rod was used as a seed, the Laue patterns of the first 25 mm of the growth (region I) show that this region is either polycrystalline or poor quality crystal. We then note that identical Laue patterns were observed in region II for ~30 mm, whereas our Laue examination of the boule at around 55 mm of growth reveals the presence of two overlapping grains extending over a short length of ~15 mm (region III) in the boule. For the remaining 15 mm of the boule (region IV), the Laue photographs show the existence of a single grain. The Laue patterns indicate that the c^* axis direction is nearly orthogonal to the growth direction.

Phase purity analysis was carried out on a ground crystal piece of $Er_2Si_2O_7$, and the powder X-ray diffraction pattern is shown in Figure 4. Profile matching (GOF = 2.57) using the Fullprof software suite[38] indicates that the main phase is the monoclinic ($P2_1/b$) D-type $Er_2Si_2O_7$. There is no evidence that the monoclinic $C2/c$ B-type Er_2SiO_5 phase is present in the crystal, although it was observed as an impurity in the starting polycrystalline powders. The lattice parameters calculated from the profile matching were determined to be a = 4.6908(2) Å, b = 5.5615(2) Å, and c = 10.7991(2) Å, with the angle γ = 96.040(2)°. These are in reasonable agreement with previously published results.[2]

Composition analysis by EDAX was performed on a cleaved piece from the $Er_2Si_2O_7$ crystal boule. This showed the cationic ratio averages of 1:1 for Er/Si for the bulk of the crystal. The average atomic percentages of Er, Si, and O were 14.4(1)%, 17.6(3)%, and 68.0(3)%, respectively. Given the limitations of this technique, the results are in reasonable agreement with the expected theoretical values of 18.2% for Er and Si, and 63.6% for O respectively.

Heat Capacity. D-Type $Er_2Si_2O_7$ orders magnetically below 1.9(1) K, with a presumed four-sublattice antiferromagnetic arrangement of Ising-like moments.[36,37] Heat capacity measurements performed in zero applied magnetic field on
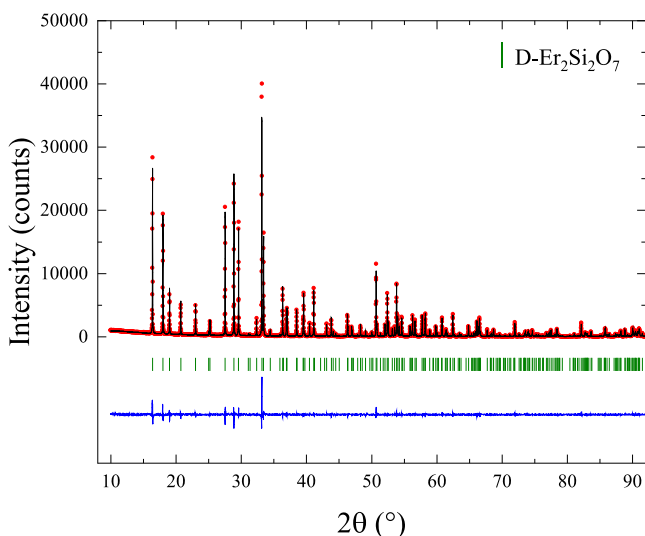
Figure 4. Room temperature powder X-ray diffraction pattern of a ground $Er_2Si_2O_7$ crystal piece. The experimental profile (red closed circles) and a full profile matching refinement (black solid line) made using the D-type $(P2_1/b)$ monoclinic structure are shown, with the difference given by the blue solid line.

an unaligned fragment of an erbium disilicate crystal show a sharp peak in $C(T)/T$ at 1.80(2) K (see Figure 5), confirming
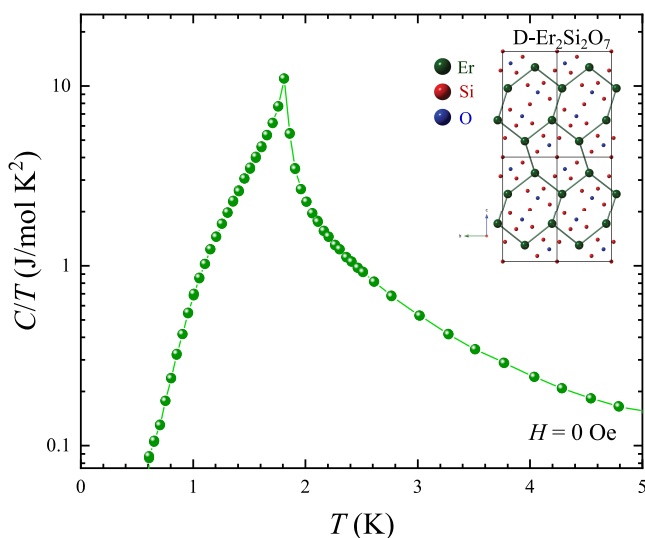

Figure 5. Temperature dependence of C/T for a D-type $Er_2Si_2O_7$ crystal piece in a zero applied magnetic field. The inset shows the arrangement of the Er^{3+} magnetic ions in the D-type crystallographic structure, emphasizing the presence of distorted honeycombs.

the ordering of the magnetic ions Er^{3+}. The temperature of the sharp feature observed in the heat capacity measurements further demonstrates that the FZ-grown $Er_2Si_2O_7$ crystal belongs to the structural type D, because C-type $Er_2Si_2O_7$ orders below $T_N = 2.50(5)$ K.[22,24] The results are in agreement with the previous results published on a $Er_2Si_2O_7$ crystal grown using the FZ method.[16] Extensive studies of the magnetic ground state of D-type $Er_2Si_2O_7$ are described elsewhere in a more detailed paper.[40]

$Ho_2Si_2O_7$. *Polycrystalline Synthesis.* The two structural types of holmium disilicate that are promising from a magnetic point of view are the C and D polymorphs. The magnetic ions

are arranged in these crystallographic structures in such a way that they form a distorted honeycomb-like lattice (see Figure 1b−c).

$Ho_2Si_2O_7$ was first prepared in polycrystalline form by the conventional solid state synthesis method. Because the temperatures of the structural phase transitions are close to one another,[2,33] we have carried out several synthesis attempts in order to determine the optimal conditions for preparing C- or D-type holmium disilicate compounds.

In a first attempt (sample labeled HSO_1), stoichiometric amounts of Ho_2O_3 and SiO_2 powders were ground together and reacted in air for several days (in four steps) at 1300 °C, with intermediate grindings. Analysis (GOF = 3.81) of the X-ray diffraction pattern collected at room temperature on this powder (see Figure 6a) indicates that the main phase is the D-type $Ho_2Si_2O_7$. Nevertheless, there are several Bragg peaks that could not be indexed with the monoclinic $(P2_1/b)$ space group and arise due to the presence of a holmium monosilicate impurity, Ho_2SiO_5. This impurity phase is present in two structural types, a monoclinic $(P2_1/c)$ structure (A-type) and a monoclinic $(C2/c)$ arrangement (B-type).[41]

The difficulty in stabilizing the Si-rich phase, $Ho_2Si_2O_7$, is probably due to the reactivity of the starting silica powder. Felsche previously reported the synthesis of rare-earth disilicates starting with the highly reactive form of SiO_2, cristobalite, a very high temperature polymorph of quartz.[2] In all our synthesis experiments, we have used a less reactive form of silica. To overcome this drawback, one option is to preanneal the starting reagent, silica, in air at high temperatures (1500−1650 °C); however, this process does not produce a direct conversion to cristobalite.[42] We have thus opted for a second solution, i.e., the synthesis using an excess of SiO_2.

An excess of 15% silica was added to the reacted stoichiometric powder obtained previously. The powder mixture was then heated in air for several days (in one step) at 1300 °C. Phase purity analysis was carried out, and the diffractogram is shown in Figure 6b. Profile matching (GOF = 3.71) indicates that the main phase is D-type $Ho_2Si_2O_7$ and that there are two impurity phases present, unreacted SiO_2 crystallizing in a tetragonal $(P4_12_12)$ structure (α-cristobalite[43]) and B-type Ho_2SiO_5. To ensure good homogeneity and to facilitate the reaction, another annealing was carried out for several days at 1300 °C. Room temperature powder X-ray diffraction measurements were again performed to determine the phase purity of the polycrystalline material. The X-ray diffraction pattern (see Figure 6c) (GOF = 6.46) reveals the presence of D-type $Ho_2Si_2O_7$, α-cristobalite, and B-type Ho_2SiO_5. In addition, a fourth chemical phase is present (indicated by the existence of one unindexed Bragg peak at ∼29.1° in 2θ); however, this impurity could not be identified, due to the reduced intensity of the peak. Two additional shoulders can be observed at ∼20.5 and 21.7° in 2θ; however, because of their extremely reduced intensities, their presence could not be correlated with any known chemical phase. Additional trials were therefore performed in order to optimize the synthesis conditions and obtain pure phase D-type $Ho_2Si_2O_7$ polycrystalline material.

In a second attempt, we have prepared three samples (labeled HSO_2, HSO_3, and HSO_4) starting with stoichiometric amounts of Ho_2O_3 and different amounts of excess SiO_2 (13, 14, and 15%). The starting oxides were mixed together and heat treated in air for several days (in two steps) at 1400 °C, with an intermediate grinding. The powder X-ray
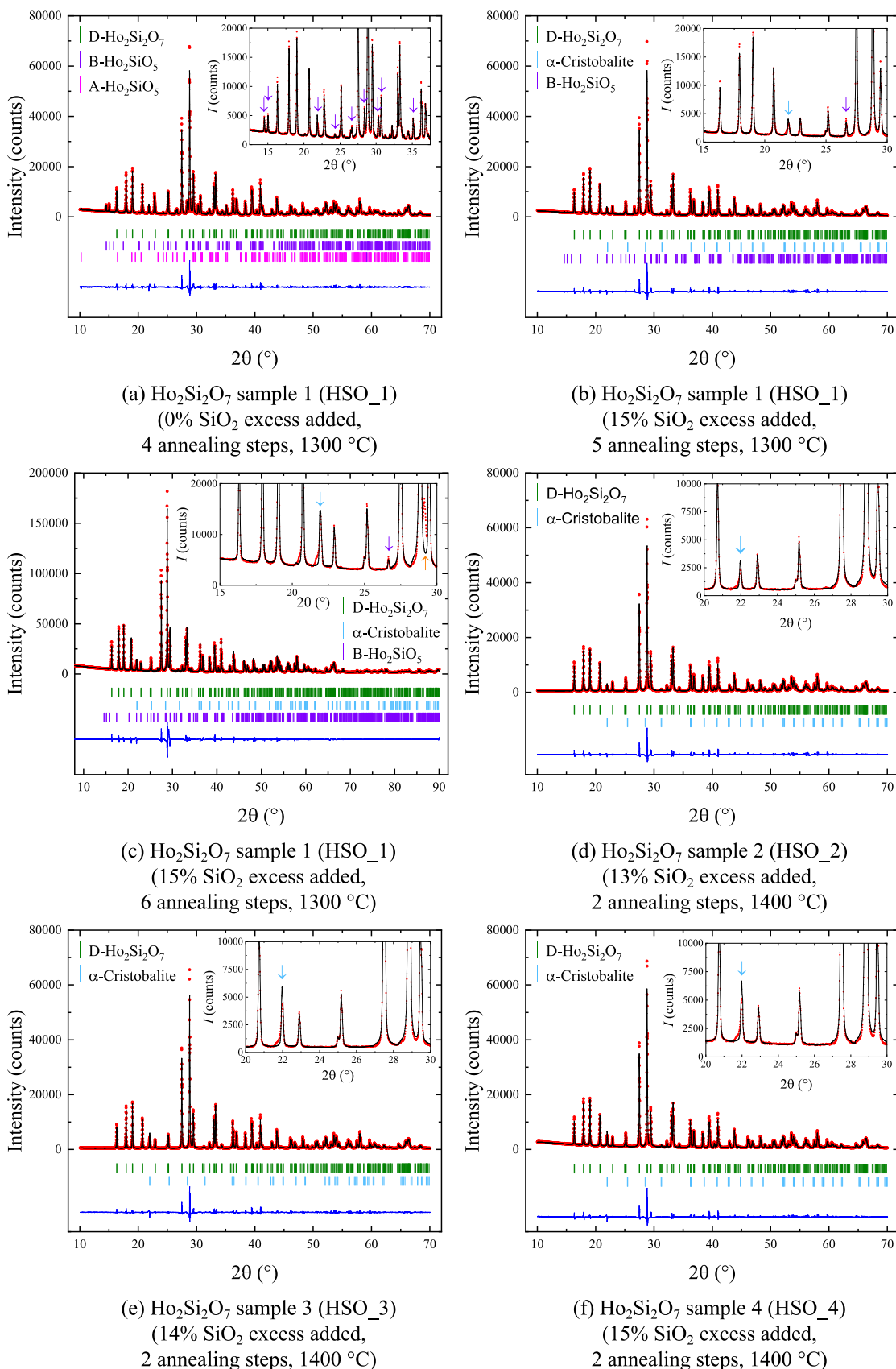
(a) $Ho_2Si_2O_7$ sample 1 (HSO_1)
(0% SiO_2 excess added,
4 annealing steps, 1300 °C)

(b) $Ho_2Si_2O_7$ sample 1 (HSO_1)
(15% SiO_2 excess added,
5 annealing steps, 1300 °C)

(c) $Ho_2Si_2O_7$ sample 1 (HSO_1)
(15% SiO_2 excess added,
6 annealing steps, 1300 °C)

(d) $Ho_2Si_2O_7$ sample 2 (HSO_2)
(13% SiO_2 excess added,
2 annealing steps, 1400 °C)

(e) $Ho_2Si_2O_7$ sample 3 (HSO_3)
(14% SiO_2 excess added,
2 annealing steps, 1400 °C)

(f) $Ho_2Si_2O_7$ sample 4 (HSO_4)
(15% SiO_2 excess added,
2 annealing steps, 1400 °C)

Figure 6. (a−f) Room temperature powder X-ray diffraction patterns of four $Ho_2Si_2O_7$ polycrystalline samples (HSO_1, HSO_2, HSO_3, and HSO_4) made using different amounts of excess SiO_2. The experimental profile (red closed circles) and a full profile matching refinement (black solid line) made using the monoclinic ($P2_1/b$) D-type structure are shown, with the difference given by the blue solid line. The reflections of the D-type $Ho_2Si_2O_7$ structure are indicated by green "|"; purple "|" show the reflections belonging to a B-type Ho_2SiO_5 (monoclinic $C2/c$ structure) impurity; pink "|" mark the reflections belonging to A-type Ho_2SiO_5 (monoclinic $P2_1/c$ structure) impurity; light blue "|" identify the Bragg peaks

Figure 6. continued

belonging to unreacted SiO_2 crystallizing in a tetragonal ($P4_12_12$) structure (α-cristobalite). The insets show the X-ray patterns over a reduced range of the scattering angle 2θ, with the impurity reflections marked by colored arrows. In (c), an orange arrow marks the reflection belonging to an impurity phase that could not be identified.

diffraction patterns obtained for the holmium disilicate powders prepared using excess silica are shown in Figure 6d−f. An analysis of the patterns provided a good fit (GOF = 3.71, 3.70, and 3.75 for 13, 14, and 15% excess SiO_2 respectively) to the D-type $Ho_2Si_2O_7$. Additionally, in all three patterns, there is one Bragg peak that could not be indexed with the monoclinic ($P2_1/b$) space group. This Bragg peak is attributed to the presence of a small amount of unreacted SiO_2, in the form of α-cristobalite. In addition, the existence of an unindexed shoulder at ∼21.7° in 2θ suggests the presence of a third chemical phase; however, this impurity could not be identified due to the reduced intensity of the peak. The best results in the synthesis of D-type $Ho_2Si_2O_7$ powders were obtained when an excess of 13% silica was used (see Figure 6d).

Throughout the synthesis procedure, extra care has been taken to minimize the amount of unreacted SiO_2 in the polycrystalline material used to prepare the feed and seed rods. To ensure a higher reactivity of the starting silica reagent, silica was preannealed in air at 1400 °C for 24 h. To ensure that the chemical reaction is complete, we have started with a slightly larger amount of excess (14%) than determined previously to be optimal, and we have reacted the powder mixtures in air for several days (in three steps). The sintered material was isostatically pressed into rods (typically 6−8 mm diameter and 70−80 mm long) and sintered at 1400−1450 °C in air for several days. The annealed rods were then used for the crystal growth.

Crystal Growth. We have first grown crystal boules of $Ho_2Si_2O_7$ using the FZ method, in a static air atmosphere, at ambient pressure. The crystal growths were carried out at growth rates in the range 5−15 mm/h, and the feed and seed rods were counter-rotated, each at a rate of 15−25 rpm. Polycrystalline rods were used as seed rods. $Ho_2Si_2O_7$ appears to melt congruently, and no deposition was observed on the quartz tube surrounding the feed and seed rods. The crystals did not develop any facets as they grew, and the crystal boules of holmium disilicate were very fragile. X-ray Laue photographs taken of these boules of $Ho_2Si_2O_7$ reveal a poor crystalline quality of the crystal boules.

The crystal growth of $Ho_2Si_2O_7$ was also carried out in air at pressures in the range 1−2 bar and a flow of air of 0.1−0.2 L/min. A growth rate of 8 mm/h was used, with the feed and seed rods counter-rotating at a rate of 10 and 25 rpm, respectively. A boule prepared in a static air atmosphere, at a growth rate of 15 mm/h was used as a seed for this crystal growth. The $Ho_2Si_2O_7$ crystal boule obtained was 5 mm in diameter and 75 mm long. The boule tended to have thermally generated cracks, and it developed facets as it grew, and two very strong facets were present on more than half the length of the grown boule. All the holmium disilicate crystal boules obtained were a pale orange color. Figure 7 shows a photograph of a crystal boule of $Ho_2Si_2O_7$, grown in air atmosphere, at pressures in the range 1−2 bar, in a flow of air of 0.1−0.2 L/min, using a growth speed of 8 mm/h. X-ray Laue photographs taken of this boule of $Ho_2Si_2O_7$ show that the crystal boule consists of a collection of several grains.

Figure 7. Boule of $Ho_2Si_2O_7$ prepared by the floating zone method in an air atmosphere, at pressures in the range 1−2 bar, in a flow of air of 0.1−0.2 L/min, using a growth speed of 8 mm/h. Also shown is the X-ray Laue pattern of one of the sides of the $Ho_2Si_2O_7$ crystal boule.

Nevertheless, long needle-like single crystals, ∼20 × 2 × 1−2 mm^3, could be isolated from the crystal boule. The size of these crystals makes them suitable for the study of the magnetic behavior of this system.

Holmium disilicate does not melt below 1750 °C, and the D → E-type structural phase transition occurs at a lower temperature than the melting point.[2] One thus expects a crystal of $Ho_2Si_2O_7$ grown using the FZ method to crystallize in the structural type stable at the highest temperature ($T \geq$ 1500 °C), i.e., E-type. Phase purity analysis of a ground piece of the holmium disilicate crystal boule grown in an air atmosphere, at pressures in the range 1−2 bar, a flow of air of 0.1−0.2 L/min, using a growth rate of 8 mm/h (see Figure 8),
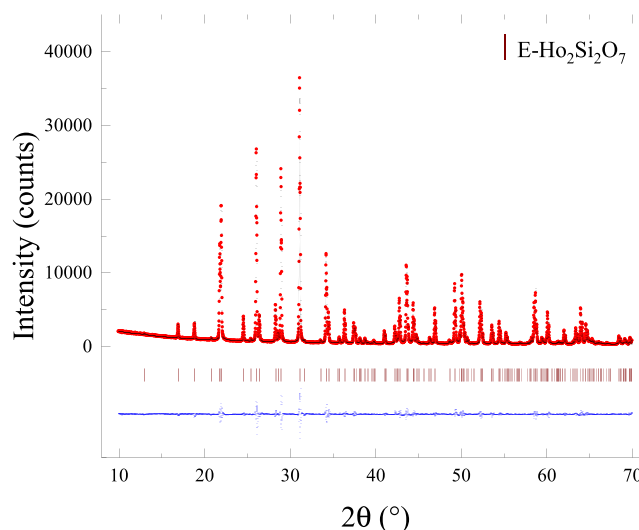

Figure 8. Room temperature powder X-ray diffraction pattern of a ground piece of $Ho_2Si_2O_7$ crystal. The experimental profile (red closed circles) and a full profile matching refinement (black solid line) made using the E-type ($Pna2_1$) orthorhombic structure are shown, with the difference given by the blue solid line.

shows that the main phase is E-type $Ho_2Si_2O_7$ (orthorhombic $Pna2_1$ structure), with no significant impurity phases present. Profile matching (GOF = 2.98) was carried out, and the lattice parameters were determined to be a = 13.6770(3) Å, b = 5.0235(3) Å, and c = 8.1598(3) Å. These are slightly smaller than the previously published results on flux grown crystals of E-type $Ho_2Si_2O_7$.[2,33]

Composition analysis by EDAX was performed on a cleaved piece from the $Ho_2Si_2O_7$ crystal boule. Given the limitations of this analysis method, the average atomic percentages of

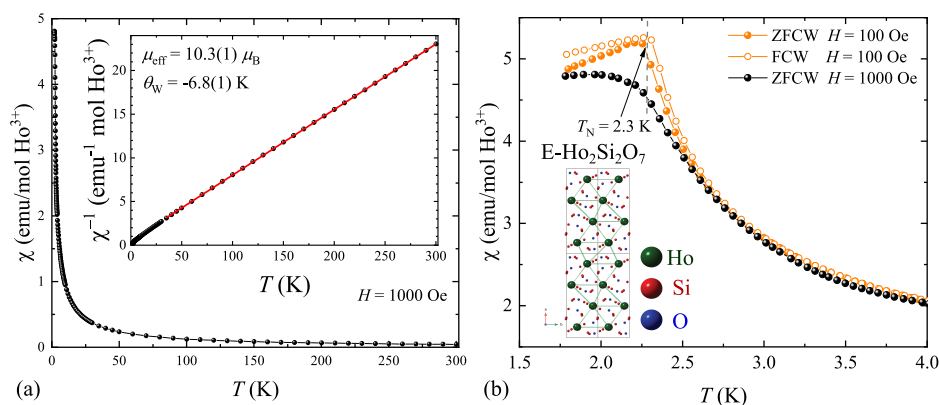**Figure 9.** (a) Temperature dependence of the *dc* magnetic susceptibility, χ, in the range 1.8−300 K for an E-type $Ho_2Si_2O_7$ ground crystal sample in an applied magnetic field of 1000 Oe. The inset shows χ^{-1} versus T and the fit using the Curie−Weiss law to the data in the temperature range 35−300 K. (b) Magnetic susceptibility data in a reduced temperature range (1.8−4 K) in applied magnetic fields of 100 and 1000 Oe. The inset shows the arrangement of the Ho^{3+} magnetic ions in the E-type crystallographic structure.

16.0(6)%, 16.6(2)%, and 67.4(6)% for Ho, Si, and O, respectively, are in reasonable agreement with the expected theoretical values (18.2% for Ho and Si, and 63.6% for O) for the $Ho_2Si_2O_7$ phase.

Magnetisation. Zero-field-cooled-warming (ZFCW) and field-cooled-warming (FCW) magnetization versus temperature curves were measured on a ground piece of the E-type $Ho_2Si_2O_7$. The temperature dependence of the *dc* magnetic susceptibility, $\chi(T)$, and reciprocal *dc* magnetic susceptibility $\chi^{-1}(T)$ are shown in Figure 9. The magnetic susceptibility in an applied magnetic field of 1000 Oe exhibits a monotonic increase when cooling from 300 to 1.8 K, and an anomaly is observed at low temperature. A fit of the $\chi^{-1}(T)$ data to a Curie−Weiss law over an extended temperature range (35−300 K) (see Figure 9a inset) shows that for $35 \leq T \leq 300$ K, E-type $Ho_2Si_2O_7$ has an effective moment of $\mu_{eff} = 10.3(1)\mu_B$ and a Weiss temperature of $\theta_W = -6.8(1)$ K. The effective moment of Ho^{3+} in holmium disilicate is in agreement with the magnetic moment of a free Ho^{3+} in the ground state $^5I_8$. The θ_W value indicates an antiferromagnetic coupling between the Ho spins.

A measurement of the temperature dependence of the susceptibility was also performed in an applied magnetic field of 100 Oe. The examination of the magnetization at low temperatures (1.8 < T < 4 K) reveals a bifurcation of the ZFCW and FCW susceptibility curves below ∼2.55(5) K, shown in Figure 9b. The feature centered around 2.30(5) K suggests the antiferromagnetic ordering between the Ho^{3+} ions. In order to establish the magnetic structure of E-type $Ho_2Si_2O_7$ and its evolution with the applied magnetic field, detailed studies of the magnetic behavior of this system are in progress.

$Tm_2Si_2O_7$. *Polycrystalline Synthesis.* The $Tm_2Si_2O_7$ polymorph stable at high temperature is C-type (see Figure 1b). The arrangement of the magnetic ions in the crystallographic structure is similar to what is observed in $Yb_2Si_2O_7$, and this motivated us to embark on the study of C-type thulium disilicate.

To prepare C-type $Tm_2Si_2O_7$ powders, stoichiometric amounts of Tm_2O_3 and SiO_2 were thoroughly ground, pressed into pellets, and then heated several times in air, for several days, at 1400 °C, above the B → C-type structural phase transition temperature,[2] in five steps, with intermediate grinding. A powder X-ray diffraction measurement was carried out at room temperature in order to check the composition of

the thulium disilicate polycrystalline sample prepared (labeled TSO_1). Analysis of the pattern (GOF = 7.26) using the FullProf software suite indicates that, although the main phase is the monoclinic ($C2/m$) C-type structure of $Tm_2Si_2O_7$, there are several peaks belonging to a thulium monosilicate impurity, Tm_2SiO_5 (see Figure 10a). This impurity is present in two structural phases, a monoclinic ($P2_1/c$) structure (A-type) and a monoclinic ($C2/c$) arrangement (B-type).[44,45]

To obtain single phase polycrystalline material of C-type $Tm_2Si_2O_7$, we have adopted a similar approach to the one used for the synthesis of $Ho_2Si_2O_7$. An excess (∼17%) of SiO_2 was added to the prereacted stoichiometric powder obtained. The powder mixture was then pressed into pellets and heated in air for several days (in one step) at 1400 °C. The X-ray diffraction pattern (GOF = 7.45) collected on this powder shows that the polycrystalline material is a mixture of phases (see Figure 10b). The main phase is C-type $Tm_2Si_2O_7$, but there are several impurity peaks belonging to A and B-type Tm_2SiO_5, as well as unreacted SiO_2 crystallized in the α-cristobalite tetragonal ($P4_12_12$) structure. The powder mixture was pelletized again and reacted in air for several days at 1400 °C. Phase purity analysis of the resulting powder by X-ray diffraction (GOF = 7.73) shows the existence of three phases, C-type $Tm_2Si_2O_7$, B-type Tm_2SiO_5, and α-cristobalite. Figure 10a−c shows that the amount of the Tm_2SiO_5 impurity is significantly reduced due to the addition of SiO_2.

A larger amount of polycrystalline sample of C-type $Tm_2Si_2O_7$ was prepared using a stoichiometric amount of Tm_2O_3 and ∼17% excess SiO_2. The starting materials were mixed together and heat treated in air for several days (in three steps) at 1400 °C, with an intermediate grinding. The sintered material (sample labeled TSO_2) was then isostatically pressed into a rod (7 mm diameter and 60 mm long) and sintered at 1400 °C in air for several days. The annealed rod was then used for the crystal growth. An analysis (GOF = 1.51) of the powder X-ray diffraction pattern collected on a ground piece of the feed rod reveals the presence of two phases, C-type $Tm_2Si_2O_7$ and B-type Tm_2SiO_5 (see Figure 10d).

The results of our synthesis experiments suggest that the stabilization of the disilicate phase in the case of thulium is more difficult than for the two other rare-earth disilicate compounds investigated in this study. This is most likely due
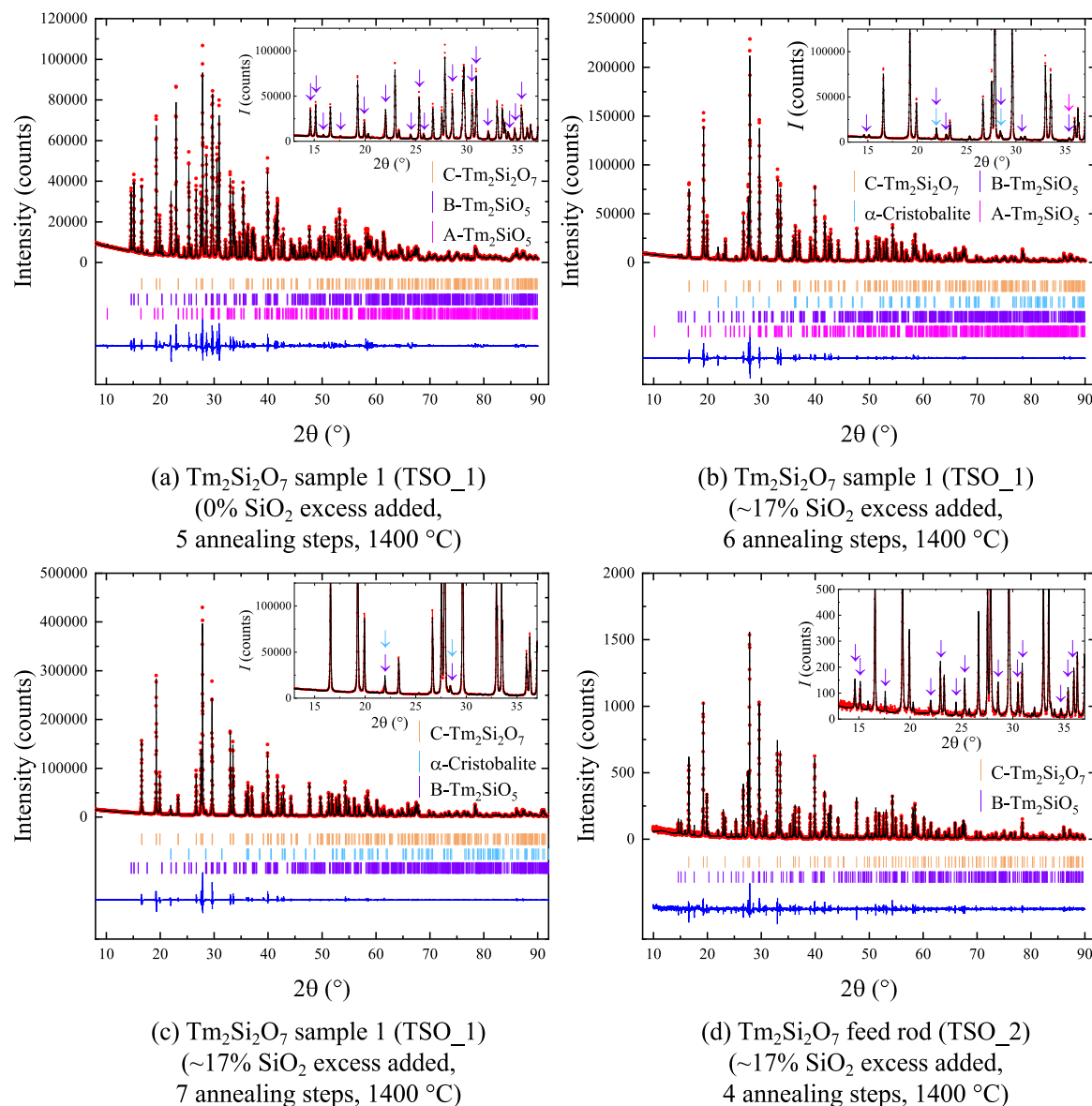
(a) Tm$_2$Si$_2$O$_7$ sample 1 (TSO_1)
(0% SiO$_2$ excess added,
5 annealing steps, 1400 °C)

(b) Tm$_2$Si$_2$O$_7$ sample 1 (TSO_1)
(~17% SiO$_2$ excess added,
6 annealing steps, 1400 °C)

(c) Tm$_2$Si$_2$O$_7$ sample 1 (TSO_1)
(~17% SiO$_2$ excess added,
7 annealing steps, 1400 °C)

(d) Tm$_2$Si$_2$O$_7$ feed rod (TSO_2)
(~17% SiO$_2$ excess added,
4 annealing steps, 1400 °C)

Figure 10. (a−d) Room temperature powder X-ray diffraction pattern of two Tm$_2$Si$_2$O$_7$ polycrystalline samples (TSO_1 and TSO_2) made with and without excess SiO$_2$. The experimental profile (red closed circles) and a full profile matching refinement (black solid line) made using the monoclinic ($C2/m$) C-type structure are shown, with the difference given by the blue solid line. The reflections of the C-type Tm$_2$Si$_2$O$_7$ structure are indicated by orange "|"; purple "|" show the reflections belonging to a B-type Tm$_2$SiO$_5$ (monoclinic $C2/c$ structure) impurity; pink "|" mark the reflections belonging to A-type Tm$_2$SiO$_5$ (monoclinic $P2_1/c$ structure) impurity; light blue "|" identify the Bragg peaks belonging to unreacted SiO$_2$ crystallizing in a tetragonal ($P4_12_12$) structure (α-cristobalite). The insets show the X-ray patterns over a reduced range of the scattering angle 2θ, with the impurity reflections marked by colored arrows.

to the very similar temperature stability ranges of Tm$_2$SiO$_5$ and Tm$_2$Si$_2$O$_7$ phases.[2,3]

Crystal Growth. We have first grown a Tm$_2$Si$_2$O$_7$ crystal boule, in a static air atmosphere, at ambient pressure, using growth rates in the range 5−7 mm/h. The feed and seed rods were counter-rotated, each at a rate of 15 rpm. A polycrystalline rod was used as a seed rod. No deposition was observed on the quartz tube surrounding the feed and seed rods, suggesting that Tm$_2$Si$_2$O$_7$ melts congruently. The crystal did not develop any facets, and the crystal boule was very fragile. To minimize the thermal stress on the crystal boule and reduce the cracks, the rotation of the seed rod was reduced to 5 rpm. Analysis by X-ray Laue diffraction of the crystalline quality of the Tm$_2$Si$_2$O$_7$ crystal boule obtained revealed the presence of multiple grains.

A second crystal growth was performed, using as feed the crystal boule obtained previously. The growth was carried out in air atmosphere, at ambient pressure, in a flow of air of 1−2 L/min, using a growth rate of 10 mm/h (see Figure 11). The feed and seed rods were counter-rotated, each at a rate of 15−

Figure 11. Boule of Tm$_2$Si$_2$O$_7$ prepared by the floating zone method in air atmosphere, at ambient pressure, in a flow of air of 1−2 L/min, using a growth speed of 10 mm/h. Also shown is the X-ray Laue pattern of one of the sides of the Tm$_2$Si$_2$O$_7$ crystal boule.

25 rpm. The $Tm_2Si_2O_7$ crystal boule obtained was ∼5 mm in diameter and 50 mm long. Thermally generated cracks were observed on the surface of the crystal boule. One facet developed midway during the growth and extended over the remaining length of the grown crystal boule. The thulium disilicate crystal boule obtained was a pale green color. A visual inspection of the cross-section of the crystal revealed that the boule consists of a semitransparent shell and an opaque core. Analysis of the X-ray Laue diffraction patterns collected along the sides of this boule of $Tm_2Si_2O_7$ shows the presence of several grains. Nonetheless, long needle-like single crystals, ∼ 10−15 × 2 × 1−2 mm^3, could be isolated from the outermost layer of the crystal boule. These crystals are suitable for magnetic properties measurements of this material.

Phase composition analysis by powder X-ray diffraction (GOF = 1.50) of a ground cross-section of $Tm_2Si_2O_7$ boule (made up of both the outer layer and the inner core) reveals that, although the main phase is C-type $Tm_2Si_2O_7$, there is a small amount of B-type Tm_2SiO_5 impurity present in the crystal (see Figure 12). The lattice parameters of monoclinic

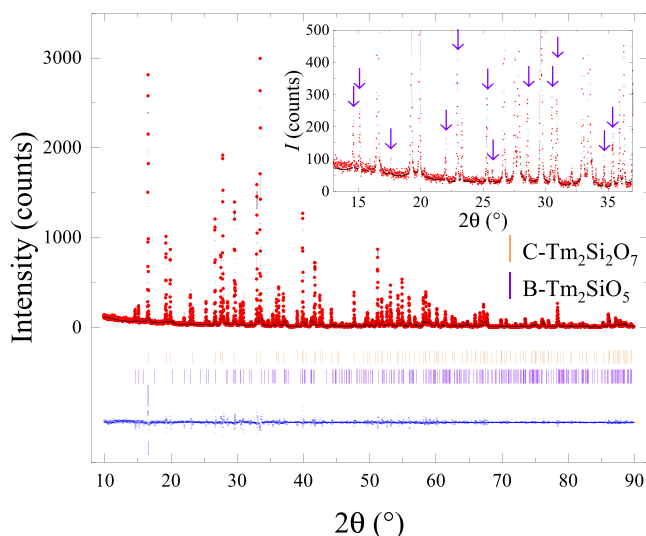**Figure 12.** Room temperature powder X-ray diffraction pattern of a ground $Tm_2Si_2O_7$ crystal piece. The experimental profile (red closed circles) and a full profile matching refinement (black solid line) made using the C-type ($C2/m$) monoclinic structure are shown, with the difference given by the blue solid line. The reflections of the C-type $Tm_2Si_2O_7$ structure are indicated by orange "|"; purple "|" show the reflections belonging to a B-type Tm_2SiO_5 (monoclinic $C2/c$ structure) impurity. The inset shows the X-ray pattern in a reduced range of the scattering angle 2θ, with the impurity reflections marked by colored arrows.

($C2/m$) thulium disilicate were determined to be a = 6.8276(2) Å, b = 8.9105(3) Å, and c = 4.7067(2) Å, with the angle β = 101.834(2)°. These values are close to the previously published results on flux grown crystals of C-type $Tm_2Si_2O_7$.[2,25]

Composition analysis by EDAX was performed on a cleaved piece from the $Tm_2Si_2O_7$ crystal boule. The average atomic percentages of Tm, Si, and O were 17.1(2)%, 16.7(2)%, and 66.2(3)% respectively. Given the limitations of this technique, the results are in reasonable agreement with the expected cationic ratio average of 1:1 for Tm/Si for the $Tm_2Si_2O_7$ phase.

The problems encountered in the preparation of $Tm_2Si_2O_7$ samples, both in powder and crystal form, are most likely due

to the similar ranges of thermal stability of the thulium monoslicate and disilicate, as well as, to the similar melting temperatures of these compounds (see, for example, the Y−Si−O system[46]). Polycrystalline and single crystal synthesis experiments are in progress in order to optimize the conditions and obtain phase C-type $Tm_2Si_2O_7$ samples.

Heat Capacity. To date, the magnetic properties of C-type $Tm_2Si_2O_7$ have not been studied. Figure 13 shows the heat

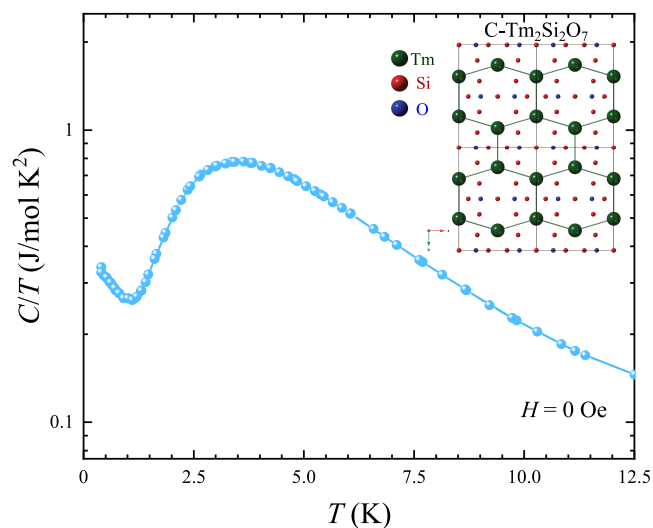**Figure 13.** $C(T)/T$ for a C-type $Tm_2Si_2O_7$ crystal piece in zero applied magnetic field. The inset shows the arrangement of the Tm^{3+} magnetic ions in the C-type crystallographic structure, emphasizing the presence of distorted honeycombs.

capacity measurement performed in zero applied magnetic field on an unaligned fragment of a thulium disilicate crystal. Similar to what is observed for C-type $Yb_2Si_2O_7$, there is no sign of magnetic ordering of $Tm_2Si_2O_7$ down to ∼0.4 K. The broad peak centered around 3.5 K corresponds, in all likelihood, to a Schottky anomaly. The increase of $C(T)/T$ below 1 K suggests the development of short-range magnetic correlations. Detailed investigations at low temperature are being carried out in order to establish the magnetic structure of C-type $Tm_2Si_2O_7$.

■ SUMMARY AND CONCLUSIONS

Samples of $R_2Si_2O_7$ (with R = Er, Ho, and Tm) compounds were first prepared in polycrystalline form by the conventional solid state synthesis method. The analysis by powder X-ray diffraction of the polycrystalline samples prepared revealed the presence of impurities (in the case of holmium and thulium), in the form of R_2SiO_5. We have shown that, to reduce the formation of the impurity monosilicate phases in the synthesis, it is necessary to start with an excess of SiO_2. Our synthesis efforts with excess SiO_2 succeeded in producing samples with considerably reduced levels of the impurity phases, and we were able to obtain mainly the desired $R_2Si_2O_7$ phase. Detailed studies are now being carried out to further optimize the synthesis conditions in order to obtain phase pure powder samples of the rare-earth disilicate compounds, minimizing the amount of unreacted SiO_2. The conditions used for the synthesis of the polycrystalline materials, as well as the results of the phase composition analysis of each sample, are summarized in Table 2.

Table 2. Summary of the Conditions Used for the Preparation of the $R_2Si_2O_7$ (with R = Er, Ho, and Tm) Polycrystalline Samples[a]

chemical composition	sample label	sintering temperature (°C)	synthesis steps number	SiO$_2$ excess (%)	phase composition analysis
Er$_2$Si$_2$O$_7$	ESO	1400−1500	4	0	mainly monoclinic D-type Er$_2$Si$_2$O$_7$ and a few peaks of monoclinic B-type Er$_2$SiO$_5$
Ho$_2$Si$_2$O$_7$	HSO_1	1300	4	0	mixture of monoclinic D-type Ho$_2$Si$_2$O$_7$, monoclinic A-type Ho$_2$SiO$_5$ and monoclinic B-type Ho$_2$SiO$_5$
	HSO_1	1300	5	15	mainly monoclinic D-type Ho$_2$Si$_2$O$_7$, a few peaks of monoclinic B-type Ho$_2$SiO$_5$ and α-cristobalite SiO$_2$
	HSO_1	1300	6	15	mainly monoclinic D-type Ho$_2$Si$_2$O$_7$, one strong peak of α-cristobalite SiO$_2$, one peak of monoclinic B-type Ho$_2$SiO$_5$, and one peak belonging to an unidentified impurity phase
	HSO_2	1400	2	13	mainly monoclinic D-type Ho$_2$Si$_2$O$_7$ and one small peak of α-cristobalite SiO$_2$
	HSO_3	1400	2	14	mainly monoclinic D-type Ho$_2$Si$_2$O$_7$ and one peak of α-cristobalite SiO$_2$
	HSO_4	1400	2	15	mainly monoclinic D-type Ho$_2$Si$_2$O$_7$ and one peak of α-cristobalite SiO$_2$
Tm$_2$Si$_2$O$_7$	TSO_1	1400	5	0	mixture of monoclinic C-type Tm$_2$Si$_2$O$_7$, monoclinic A-type Tm$_2$SiO$_5$, and monoclinic B-type Tm$_2$SiO$_5$
	TSO_1	1400	6	17	mainly monoclinic C-type Tm$_2$Si$_2$O$_7$, a few strong peaks of monoclinic monoclinic B-type Tm$_2$SiO$_5$, and a few peaks of A-type Tm$_2$SiO$_5$ and α-cristobalite SiO$_2$
	TSO_1	1400	7	17	mainly monoclinic C-type Tm$_2$Si$_2$O$_7$ and a few peaks of monoclinic monoclinic B-type Tm$_2$SiO$_5$ and α-cristobalite SiO$_2$
	TSO_2	1400	4	17	mainly monoclinic C-type Tm$_2$Si$_2$O$_7$ and a few peaks of monoclinic monoclinic B-type Tm$_2$SiO$_5$

[a]All the samples were sintered for a duration of 48−96 h per step. The results of the phase composition analysis by powder X-ray diffraction are given for each sample.

Table 3. Summary of the Conditions Used for the Growth of $R_2Si_2O_7$ (with R = Er, Ho, and Tm) Crystal Boules[a]

R$_2$Si$_2$O$_7$	growth rate (mm/h)	gas atmosphere/pressure/flow	feed and seed rotation rate (rpm)	remarks
Er$_2$Si$_2$O$_7$	5−12	air, ambient	10−25	cloudy pink boules
	10−12	air, ambient	20−25	grains ~5 × 5 × 3 mm^3*
Ho$_2$Si$_2$O$_7$	5−15	air, ambient	15−25	pale orange boules
	8	air, 1−2 bar, 0.1−0.2 L/min	10−25	grains ~20 × 2 × 1−2 mm^3*
Tm$_2$Si$_2$O$_7$	5−7	air, ambient	15−5	pale green boules
	10	air, ambient, 1−2 L/min	15−25	grains ~10−15 × 2 × 1−2 mm^3*

[a]The optimal growth conditions that allowed us to obtain better quality boules and to isolate good size single crystals fragments for characterisation measurements are marked using *.

Table 4. Lattice Parameters for $R_2Si_2O_7$ (with R = Er, Ho, and Tm), Refined from the Room Temperature Powder X-ray Diffraction Data Collected on Ground Pieces Isolated from the Crystal Boules

chemical composition	structure (type)	space group	lattice parameters			
			a (Å)	b (Å)	c (Å)	angle (°)
Er$_2$Si$_2$O$_7$	monoclinic (D)	$P2_1/b$	4.6908(2)	5.5615(2)	10.7991(2)	γ = 96.040(2)
Ho$_2$Si$_2$O$_7$	orthorhombic (E)	$Pna2_1$	13.6770(3)	5.0235(3)	8.1598(3)	
Tm$_2$Si$_2$O$_7$	monoclinic (C)	$C2/m$	6.8276(2)	8.9105(3)	4.7067(2)	β = 101.834(2)

We have been successful in growing crystals of $R_2Si_2O_7$ (with R = Er, Ho, and Tm) using the FZ method. All the rare-earth disilicate compounds appear to melt congruently, and no evaporation was observed for the growths. The crystal growths were performed using various growth rates, in air. All the rare-earth disilicate crystals are very fragile and tend to have thermally generated cracks. In general, crystal boules of better crystalline quality were obtained using average or high speed of growth. A summary of the conditions used for each crystal growth is given in Table 3.

The quality and composition of the as-grown $R_2Si_2O_7$ boules were investigated using X-ray diffraction techniques. The lattice parameters determined by powder X-ray diffraction are collected in Table 4. Erbium and holmium disilicate crystals are single phase, whereas the thulium crystal boule consists of two chemical phases (monosilicate and disilicate), due to the overlapping ranges of thermal stability of the two thulium silicate compounds, Tm_2SiO_5 and $Tm_2Si_2O_7$. The lattice

parameters of the $R_2Si_2O_7$ crystal boules are in agreement with the previously published results. Despite the difficulties encountered in the preparation of polycrystalline and crystal samples, good size grains could be isolated from the crystal boules to be used for further physical properties characterization measurements. Further investigations to better understand the stabilization of $R_2Si_2O_7$ phases in their crystal form are in progress.

Magnetic properties measurements confirm an antiferromagnetic ordering of Er^{3+} ions at T_N = 1.80(2) K in D-type $Er_2Si_2O_7$. We report, for the first time, that E-type $Ho_2Si_2O_7$ orders antiferromagnetically below T_N = 2.30(5) K. We also show that $Tm_2Si_2O_7$ exhibits no signs of long-range magnetic ordering down to ~0.4 K; however, short-range magnetic correlations develop below 1 K. Detailed magnetic properties measurements are now being carried out on the $R_2Si_2O_7$ (with R = Er, Ho, and Tm) crystals to determine the magnetic ground state of these materials.

AUTHOR INFORMATION

Corresponding Author

    Monica Ciomaga Hatnean − *Department of Physics, University of Warwick, Coventry CV4 7AL, U.K.;* ⊙ orcid.org/0000-0003-2870-8847; Email: M.Ciomaga-Hatnean@warwick.ac.uk

Authors

    Oleg A. Petrenko − *Department of Physics, University of Warwick, Coventry CV4 7AL, U.K.*

    Martin R. Lees − *Department of Physics, University of Warwick, Coventry CV4 7AL, U.K.*

    Tom E. Orton − *Department of Physics, University of Warwick, Coventry CV4 7AL, U.K.*

    Geetha Balakrishnan − *Department of Physics, University of Warwick, Coventry CV4 7AL, U.K.*

Complete contact information is available at:
https://pubs.acs.org/10.1021/acs.cgd.0c00792

Notes

The authors declare no competing financial interest.

ABBREVIATIONS

FZ, floating zone; GOF, goodness of fit.

REFERENCES

(1) Ito, J.; Johnson, H. Synthesis and study of yttrialite. *Am. Mineral.* **1968**, *53*, 1940−1952.

(2) Felsche, J. Polymorphism and crystal data of the rare-earth disilicates of type R.E.$_2$Si$_2$O$_7$. *J. Less-Common Met.* **1970**, *21*, 1−14.

(3) Felsche, J. The crystal chemistry of the rare-earth silicates. *Struct. Bonding (Berlin, Ger.)* **1973**, *13*, 99−197.

(4) Liu, X.; Fleet, M. E. High-pressure synthesis of a La orthosilicate and Nd, Gd, and Dy disilicates. *J. Phys.: Condens. Matter* **2002**, *14*, 11223−11226.

(5) Bretheau-Raynal, F.; Tercier, N.; Blanzat, B.; Drifford, M. Synthesis and spectroscopic study of lutetium pyrosilicate single crystals doped with trivalent europium. *Mater. Res. Bull.* **1980**, *15*, 639−646.

(6) Pauwels, D.; Le Masson, N.; Viana, B.; Kahn-Harari, A.; van Loef, E.; Dorenbos, P.; van Eijk, C. A novel inorganic scintillator: Lu$_2$Si$_2$O$_7$:Ce^{3+} (LPS). *IEEE Trans. Nucl. Sci.* **2000**, *47*, 1787−1790.

(7) Feng, H.; Ding, D.; Li, H.; Lu, S.; Pan, S.; Chen, X.; Ren, G. Growth and luminescence characteristics of cerium-doped yttrium pyrosilicate single crystal. *J. Alloys Compd.* **2010**, *489*, 645−649.

(8) Feng, H.; Ren, G.; Wu, Y.; Xu, J.; Yang, Q.; Xie, J.; Chou, M.; Chen, C. Optical and thermoluminescence properties of Lu$_2$Si$_2$O$_7$:Pr single crystal. *J. Rare Earths* **2012**, *30*, 775−779.

(9) Fernández-Carrión, A. J.; Allix, M.; Ocaña, M.; García-Sevillano, J.; Cusso, F.; Fitch, A. N.; Suard, E.; Becerro, A. I. Crystal Structures and Photoluminescence across the La$_2$Si$_2$O$_7$-Ho$_2$Si$_2$O$_7$ System. *Inorg. Chem.* **2013**, *52*, 13469−13479.

(10) Lee, K. N.; Fox, D. S.; Bansal, N. P. Rare earth silicate environmental barrier coatings for SiC/SiC composites and Si$_3$N$_4$ ceramics. *J. Eur. Ceram. Soc.* **2005**, *25*, 1705−1715.

(11) Sun, Z.; Zhou, Y.; Wang, J.; Li, M. Thermal Properties and Thermal Shock Resistance of γ - Y$_2$Si$_2$O$_7$. *J. Am. Ceram. Soc.* **2008**, *91*, 2623−2629.

(12) Sun, Z.; Li, M.; Zhou, Y. Thermal properties of single-phase Y$_2$SiO$_5$. *J. Eur. Ceram. Soc.* **2009**, *29*, 551−557.

(13) Zhou, Y.; Zhao, C.; Wang, F.; Sun, Y.; Zheng, L.; Wang, X. Theoretical Prediction and Experimental Investigation on the Thermal and Mechanical Properties of Bulk β - Yb$_2$Si$_2$O$_7$. *J. Am. Ceram. Soc.* **2013**, *96*, 3891−3900.

(14) Tian, Z.; Zheng, L.; Li, Z.; Li, J.; Wang, J. Exploration of the low thermal conductivities of γ - Y$_2$Si$_2$O$_7$, β - Y$_2$Si$_2$O$_7$, β - Yb$_2$Si$_2$O$_7$, and β - Lu$_2$Si$_2$O$_7$ as novel environmental barrier coating candidates. *J. Eur. Ceram. Soc.* **2016**, *36*, 2813−2823.

(15) Luo, Y.; Sun, L.; Wang, W.; Wu, Z.; Lv, X.; Wang, J. Material-genome perspective towards tunable thermal expansion of rare-earth di-silicates. *J. Eur. Ceram. Soc.* **2018**, *38*, 3547−3554.

(16) Nair, H. S.; DeLazzer, T.; Reeder, T.; Sikorski, A.; Hester, G.; Ross, K. A. Crystal Growth of Quantum Magnets in the Rare-Earth Pyrosilicate Family R$_2$Si$_2$O$_7$ (R = Yb, Er) Using the Optical Floating Zone Method. *Crystals* **2019**, *9*, 196.

(17) Hester, G.; Nair, H.; Reeder, T.; Yahne, D.; DeLazzer, T.; Berges, L.; Ziat, D.; Neilson, J.; Aczel, A.; Sala, G.; Quilliam, J.; Ross, K. Novel Strongly Spin-Orbit Coupled Quantum Dimer Magnet: Yb$_2$Si$_2$O$_7$. *Phys. Rev. Lett.* **2019**, *123*, 027201.

(18) Flynn, M. O.; Baker, T. E.; Jindal, S.; Singh, R. R. P. On two phases inside the Bose condensation dome of Yb$_2$Si$_2$O$_7$. *arXiv.org, e-Print Arch., Condens. Matter* **2020**, arXiv:2001.08219.

(19) Smolin, Y. I.; Shepelev, Y. F. The crystal structures of the rare earth pyrosilicates. *Acta Crystallogr., Sect. B: Struct. Crystallogr. Cryst. Chem.* **1970**, *26*, 484−492.

(20) Wanklyn, B. M.; Wondre, F. R.; Ansell, G. B.; Davison, W. Flux growth of rare earth silicates and aluminosilicates. *J. Mater. Sci.* **1974**, *9*, 2007−2014.

(21) Wanklyn, B. M. Effects of modifying starting compositions for flux growth. *J. Cryst. Growth* **1978**, *43*, 336−344.

(22) Maqsood, A.; Wanklyn, B. M.; Garton, G. Flux growth of polymorphic rare-earth disilicates, R$_2$Si$_2$O$_7$ (R = Tm, Er, Ho, Dy). *J. Cryst. Growth* **1979**, *46*, 671−680.

(23) Nørlund Christensen, A.; Hazell, R. G.; Hewat, A. W. Synthesis, Crystal Growth and Structure Investigations of Rare-Earth Disilicates and Rare-Earth Oxyapatites. *Acta Chem. Scand.* **1997**, *51*, 37−43.

(24) Maqsood, A. Single crystal growth of polymorphic Er$_2$Si$_2$O$_7$ ceramics. *J. Mater. Sci. Lett.* **2000**, *19*, 711−712.

(25) Kahlenberg, V.; Aichholzer, P. Thortveitite-type Tm$_2$Si$_2$O$_7$. *Acta Crystallogr., Sect. E: Struct. Rep. Online* **2014**, *70*, i34−i35.

(26) Chi, L.-S.; Chen, H.-Y.; Zhuang, H.-H.; Huang, J.-S. Synthesis and Crystal Structure of Er$_2$Si$_2$O$_7$. *Chin. J. Struct. Chem.* **1998**, *17*, 24−26.

(27) Horiai, T.; Kurosawa, S.; Murakami, R.; Pejchal, J.; Yamaji, A.; Shoji, Y.; Chani, V.; Ohashi, Y.; Kamada, K.; Yokota, Y.; Yoshikawa, A. Crystal growth and luminescence properties of Yb$_2$Si$_2$O$_7$ infra-red emission scintillator. *Opt. Mater. (Amsterdam, Neth.)* **2016**, *58*, 14−17.

(28) Balakrishnan, G.; Petrenko, O. A.; Lees, M. R.; Paul, D. M. Single crystal growth of rare earth titanate pyrochlores. *J. Phys.: Condens. Matter* **1998**, *10*, L723−L725.

(29) Koohpayeh, S. M.; Fort, D.; Abell, J. S. The optical floating zone technique: A review of experimental procedures with special reference to oxides. *Prog. Cryst. Growth Charact. Mater.* **2008**, *54*, 121−137.

(30) Dabkowska, H.; Dabkowski, A. *Handbook of Crystal Growth*, 2nd ed.; Elsevier, 2015; pp 281−329.

(31) Maqsood, A.; ul Haq, I. Preparation of rare-earth disilicates and their X-ray diffraction studies. *J. Mater. Sci. Lett.* **1987**, *6*, 1095−1097.

(32) Maqsood, A. Phase transformations in Er$_2$Si$_2$O$_7$ ceramics. *J. Mater. Sci. Lett.* **1997**, *16*, 837−840.

(33) Maqsood, A. Phase transformations in Ho$_2$Si$_2$O$_7$ ceramics. *J. Alloys Compd.* **2009**, *471*, 432−434.

(34) Ciomaga Hatnean, M.; Decorse, C.; Lees, M. R.; Petrenko, O. A.; Balakrishnan, G. Zirconate pyrochlore frustrated magnets: crystal growth by the floating zone technique. *Crystals* **2016**, *6*, 79.

(35) Sibille, R.; Lhotel, E.; Ciomaga Hatnean, M.; Nilsen, G. J.; Ehlers, G.; Cervellino, A.; Ressouche, E.; Frontzek, M.; Zaharko, O.; Pomjakushin, V.; Stuhr, U.; Walker, H. C.; Adroja, D. T.; Luetkens, H.; Baines, C.; Amato, A.; Balakrishnan, G.; Fennell, T.; Kenzelmann, M. Coulomb spin liquid in anion-disordered pyrochlore $Tb_2Hf_2O_7$. *Nat. Commun.* **2017**, *8*, 892.

(36) Maqsood, A. Magnetic properties of $D-Er_2Si_2O_7$ at low temperatures. *J. Mater. Sci.* **1981**, *16*, 2198−2204.

(37) Leask, M. J. M.; Tapster, P. R.; Wells, M. R. Magnetic properties of $D-Er_2Si_2O_7$. *J. Phys. C: Solid State Phys.* **1986**, *19*, 1173−1187.

(38) Rodríguez-Carvajal, J. Recent advances in magnetic structure determination by neutron powder diffraction. *Phys. B (Amsterdam, Neth.)* **1993**, *192*, 55−69.

(39) Phanon, D.; Černý, R. Crystal structure of the B-type dierbium oxide ortho-oxosilicate $Er_2O[SiO_4]$. *Z. Anorg. Allg. Chem.* **2008**, *634*, 1833−1835.

(40) Petrenko, O. A.; Ciomaga Hatnean, M.; Manuel, P.; Orlandi, F.; Khalyavin, D. D.; Balakrishnan, G. in preparation, 2020.

(41) Maqsood, A. Single crystal preparation of the rare earth oxyorthosilicates R_2SiO_5 (R = Er, Ho, Dy) by a flux method. *J. Mater. Sci. Lett.* **1984**, *3*, 65−67.

(42) Chaklader, A. C. D.; Roberts, A. L. Transformation of Quartz to Cristobalite. *J. Am. Ceram. Soc.* **1961**, *44*, 35−41.

(43) Downs, R. T.; Palmer, D. C. The pressure behavior of α cristobalite. *Am. Mineral.* **1994**, *79*, 9−14.

(44) Wang, J.; Tian, S.; Li, G.; Liao, F.; Jing, X. Preparation and X-ray characterization of low-temperature phases of R_2SiO_5 (R = rare earth elements). *Mater. Res. Bull.* **2001**, *36*, 1855−1861.

(45) Tian, Z.; Zheng, L.; Wang, J.; Wan, P.; Li, J.; Wang, J. Theoretical and experimental determination of the major thermo-mechanical properties of RE_2SiO_5 (RE = Tb, Dy, Ho, Er, Tm, Yb, Lu, and Y) for environmental and thermal barrier coating applications. *J. Eur. Ceram. Soc.* **2016**, *36*, 189−202.

(46) Abdul-Jabbar, N. M.; Poerschke, D. L.; Gabbett, C.; Levi, C. G. Phase equilibria in the zirconia−yttria/gadolinia−silica systems. *J. Eur. Ceram. Soc.* **2018**, *38*, 3286−3296.